

Water color from Sentinel-2 MSI data for monitoring large rivers: Yangtze and Danube

Shenglei Wang, Xuezhu Jiang, Evangelos Spyarakos, Junsheng Li, Conor McGlinchey, Adriana Maria Constantinescu & Andrew N. Tyler

To cite this article: Shenglei Wang, Xuezhu Jiang, Evangelos Spyarakos, Junsheng Li, Conor McGlinchey, Adriana Maria Constantinescu & Andrew N. Tyler (26 Sep 2023): Water color from Sentinel-2 MSI data for monitoring large rivers: Yangtze and Danube, Geo-spatial Information Science, DOI: [10.1080/10095020.2023.2258950](https://doi.org/10.1080/10095020.2023.2258950)

To link to this article: <https://doi.org/10.1080/10095020.2023.2258950>



© 2023 Wuhan University. Published by Informa UK Limited, trading as Taylor & Francis Group.



Published online: 26 Sep 2023.



Submit your article to this journal [↗](#)



Article views: 335



View related articles [↗](#)



View Crossmark data [↗](#)

Water color from Sentinel-2 MSI data for monitoring large rivers: Yangtze and Danube

Shenglei Wang^{a,b}, Xuezhu Jiang^{a,b,c}, Evangelos Spyarakos^d, Junsheng Li^{a,b,e}, Conor McGlinchey^d, Adriana Maria Constantinescu^f and Andrew N. Tyler^d

^aInternational Research Center of Big Data for Sustainable Development Goals, Beijing, China; ^bKey Laboratory of Digital Earth Science, Aerospace Information Research Institute, Chinese Academy of Sciences, Beijing, China; ^cCollege of Resources and Environment, University of Chinese Academy of Sciences, Beijing, China; ^dEarth and Planetary Observation Sciences (EPOS), Department of Biological and Environmental Studies, Faculty of Environmental Sciences, University of Stirling, Stirling, UK; ^eSchool of Electronic, Electrical and Communication Engineering, University of Chinese Academy of Sciences, Beijing, China; ^fNational Institute of Marine Geology and GeoEcology - GeoEcoMar, Bucharest, Romania

ABSTRACT

Rivers provide key ecosystem services that are inherently engineered and optimized to meet the strategic and economic needs of countries around the world. However, limited water quality records of a full river continuum hindered the understanding of how river systems response to the multiple stressors acting on them. This study highlights the use of Sentinel-2 Multi-Spectral Imager (MSI) data to monitor changes in water color in two optically complex river systems: the Yangtze and Danube using the Forel-Ule Index (FUI). FUI divides water color into 21 classes from dark blue to yellowish brown stemming from the historical Forel-Ule water color scale and has been promoted as a useful indicator showing water turbidity variations in water bodies. The results revealed contrasting water color patterns in the two rivers on both spatial and seasonal scales. Spatially, the FUI of the Yangtze River gradually increased from the upper reaches to the lower reaches, while the FUI of the Danube River declined in the lower reaches, which is possibly due to the sediment sink effect of the Iron Gate Dams. The regional FUI peaks and valleys observed in the two river systems have also been shown to be related to the dams and hydropower stations along them. Seasonally, the variations of FUI in both systems can be attributed to climate seasonality, especially precipitation in the basin and the water level. Moreover, land cover within the river basin was possibly a significant determinant of water color, as higher levels of vegetation in the Danube basin were associated with lower FUI values, whereas higher FUI values and lower levels of vegetation were observed in the Yangtze system. This study furthers our knowledge of using Sentinel-2 MSI to monitor and understand the spatial-temporal variations of river systems and highlights the capabilities of the FUI in an optically complex environment.

ARTICLE HISTORY

Received 1 February 2023

Accepted 10 September 2023

KEYWORDS

Forel-Ule Index (FUI); water color; water quality; rivers; Sentinel-2; MSI; Yangtze; Danube

1. Introduction

Rivers are critical parts of global hydrology and closely coupled with Earth's ecological and biogeochemical processes (Coss et al. 2022). They provide ecosystem services that are fundamental to societal wellbeing around the world. Human activities and climate change continue to pose threats to the river connectivity, its color and quality, and ultimate ecological status and functioning. Increased pollution from urban and agricultural areas in the river basin, sediment trapping from dam building, and the cascading hydrological and sedimentological effects of climate change can impact river connectivity, deteriorate the water quality in these already vulnerable systems, and ultimately influence their ecological status and functioning (Dethier, Renshaw, and Magilligan 2022; Reid et al. 2019). However, the nature of the impacts from

multiple stressors acting on river ecosystems is not well understood (Birk et al. 2020). Hence, monitoring the water quality conditions of the full river continuum and understanding their response to environmental changes are of considerable value in the management and protection of river systems.

The Yangtze River and Danube River have played central roles in the socioeconomic development of Asia and Europe and provide habitats for a staggering number of species. At the same time, the water quality of these two rivers has always been of a major concern for Chinese and European societies. The Yangtze River has been a source of life and prosperity for the Chinese people for centuries and is a habitat for a remarkable variety of aquatic species (Floehr et al. 2013). However, the water quality in the Yangtze River has deteriorated since the 1990s due to the rapid economic expansion in

CONTACT Evangelos Spyarakos  evangelos.spyarakos@stir.ac.uk; Junsheng Li  lijs@radi.ac.cn

© 2023 Wuhan University. Published by Informa UK Limited, trading as Taylor & Francis Group.

This is an Open Access article distributed under the terms of the Creative Commons Attribution License (<http://creativecommons.org/licenses/by/4.0/>), which permits unrestricted use, distribution, and reproduction in any medium, provided the original work is properly cited. The terms on which this article has been published allow the posting of the Accepted Manuscript in a repository by the author(s) or with their consent.

China (Yang et al. 2008). In the past decades, the Yangtze River has suffered from water pollution via urban sewage, agricultural effluent, and industrial wastewater. Furthermore, the construction of dams and reservoir sedimentation has resulted in a drastic decline in the sediment flux (77%–99%) in the Yangtze mainstream, which has a significant impact on erosion and water quality (Floehr et al. 2013; Yang et al. 2018).

The Danube River flows through much of Central and Southeastern Europe, from the Black Forest in Germany into the Black Sea, and its drainage basin includes 19 countries in Europe. Due to its economic importance, water quality in the Danube River has been a focal point of many studies. Anthropogenic activities in its catchment have intensified since the late nineteenth century (Schwarz et al. 2008). Over the last few decades, but particularly between 1950 and 1980, the Danube River faced marked declines in water quality mainly due to agriculture, industry, and construction of major dams (Panin and Jipa 2002; Sommerwerk et al. 2022). Water quality was greatly affected by the drastic decrease of wetlands area, by 80% over the second half of the twentieth century, leading to a decrease in aquatic plant biomass and flood attenuation capacity (Vadineanu et al. 2003). The sediment balance in the river and its delta was also impacted in the last century by the extent of agricultural lands, embankment for flood protection (Constantinescu et al. 2015; Hein et al. 2016), the construction of over 78 dams and reservoirs along the river (Habersack et al. 2016), and direct interventions in the delta complex (Panin and Overmars 2012).

The lack of consistent data on water quality over the length of rivers and the challenges with regard to the collection of monitoring field data are well recognized. The opportunity to unlock these challenges is only now possible with recent realizations in Earth observation and Big Earth Data cloud computing platform. These have enabled large-scale water observation capability (Hou et al. 2022; Wang et al. 2018, 2021). The increasing monitoring capabilities that recent Earth observation missions offer are now extending satellite applications to large river systems (Dethier, Renshaw, and Magilligan 2022; Guan et al. 2022). However, the complex optical properties and water constituents of inland waters hinder the development of valid Earth observation for the water quality of inland waters over large scales. Explicit spatial and temporal studies on inter-regional rivers remain very limited due to the contradiction of spatial resolution and spectral resolution of satellite data.

Water color shows the interaction outcome of sun light and water constituents, and therefore, it is directly linked with absorption and backscattering of water column. Water color has been recorded from global waters by using the traditional Forel-Ule scale for more than one century. In the era of satellite observation, water color can also be derived from the visible bands of satellite data.

Forel-Ule Index (FUI) is stemming from the Forel-Ule scale, and it classifies the natural water color into 21 classes from dark blue to yellowish brown. Studies have demonstrated that FUI is a very useful water quality indicator, which can reflect the overall water quality and turbidity for both oceans and inland waters (Garaba et al. 2015; Li et al. 2016; Pitarch et al. 2019; Wang et al. 2020). Generally, the water turns to be more turbid with higher FUI and stays clean with lower FUI (Wang et al. 2020). The calculation of FUI includes a normalization process that makes it more robust to aerosol and observational perturbations. FUI can be derived from multisource satellite data with high accuracy (Van der Woerd and Wernand 2015, 2018; Wang et al. 2014, 2021; Zhang et al. 2022). This allows for an application of FUI over a wider range of waters including global inland waters and oceans (Pitarch et al. 2021; Wang et al. 2021).

In this article, the FUI was derived for the main channel of Yangtze and Danube rivers using Sentinel-2 Multi-Spectral Imager (MSI) data during 2019–2021. For the first time, the spatial and seasonal patterns in water color of the two rivers were analyzed, and the influencing factors associated with the patterns were explored.

2. Data and methods

2.1. Sentinel-2 MSI data and preprocessing

Sentinel-2 MSI is a wide-swath, high-resolution satellite with 13 spectral bands and spatial resolutions of 10 m (visible and NIR), 20 m (red-edge and SWIR) on ground, and 60 m in the atmospheric band. Sentinel-2 consists of two satellites, Sentinel-2A and Sentinel-2B, with a revisit period of 5 days. This article utilizes Sentinel-2 Level-2A (L2A) Surface Reflection (SR) imagery of the Yangtze River and Danube River, which was obtained through Google Earth Engine (GEE). MSI images with a cloud cover of less than 20% were selected. The residual clouds were further masked using the QA60 band included in the Sentinel-2 L2A SR product. A simple correction method for satellite SR product was adopted to calculate remote sensing reflectance by subtracting the minimum value from the NIR to SWIR bands and dividing by π (Wang, Li et al. 2016; Wang et al. 2016). Studies have demonstrated that this simple correction method produced satisfactory results over a wide range of inland waters (Cao et al. 2022; Wang et al. 2018, 2020; Yin et al. 2021).

Due to variations in river channels and water volumes, the boundary of river water typically presents dynamic changes. The extraction of water from Sentinel-2 MSI data included the acquisition of the Yangtze and Danube rivers' main channels from the Global River and Lake Vector dataset (Qiu 2018). Then, a 1-km buffer was made around the main channel of the river water. Within the buffer zone, the water mask of the river water was extracted using the Modified Normalized Difference

Water Index (MNDWI). We calculated the MNDWI of Sentinel-2 images (Xu 2005) and then determined the optimal threshold value for the river according to the Otsu method (Otsu 1979). Finally, the water body mask of the river was used to determine the centerline of river water with a width greater than 100 m using the RivWidthCloud automatic extraction algorithm (Yang et al. 2019). To minimize the possible land adjacency effect, FUI calculated on the river centerline was used in the analysis.

2.2. Water color calculation

The FUI with 21 water color classes (Figure 1) was retrieved for the main river channels of Yangtze and Danube with the visible bands of Sentinel-2 MSI data after preprocessing, and the main steps can be summarized in five steps.

- (1) CIE tristimulus X , Y , and Z were calculated from the visible bands of Sentinel-2 MSI L2A data after water-leaving correction using a linear intercept method (Van der Woerd and Wernand 2018):

$$\begin{aligned} X &= 11.756R_{rs}(443) + 6.423R_{rs}(490) + 53.696R_{rs}(560) \\ &\quad + 32.028R_{rs}(665) + 0.529R_{rs}(705) \\ Y &= 1.744R_{rs}(443) + 22.289R_{rs}(490) + 65.702R_{rs}(560) \\ &\quad + 16.808R_{rs}(665) + 0.192R_{rs}(705) \\ Z &= 62.696R_{rs}(443) + 31.101R_{rs}(490) + 1.778R_{rs}(560) \\ &\quad + 0.015R_{rs}(665) + 0.000R_{rs}(705) \end{aligned} \quad (1)$$

- (2) The CIE tristimulus X , Y , and Z were normalized to obtain the chromaticity coordinates x and y as follows:

$$\begin{aligned} x &= \frac{X}{X + Y + Z} \\ y &= \frac{Y}{X + Y + Z} \end{aligned} \quad (2)$$

- (3) Hue angle α was calculated with the chromaticity coordinates x and y .

$$\alpha = (\arctan 2(y - 1/3, x - 1/3) \bmod 2\pi) * 180/\pi \quad (3)$$

- (4) Delta (Δ) correction of hue angle for eliminating the color difference caused by the visible band setting of Sentinel-2 MSI.

$$\begin{aligned} \Delta &= -65.74 * (\alpha/100)^5 + 477.16 * (\alpha/100)^4 \\ &\quad - 1279.99 * (\alpha/100)^3 + 1524.96 * (\alpha/100)^2 \\ &\quad - 751.59 * (\alpha/100) + 116.56 \end{aligned} \quad (4)$$

- (5) The FUI of each pixel can be derived with the corrected hue angle α using a FUI-hue angle look-up table following that in Wang et al. (2021).
- (6) Seasonal maps of FUI were calculated based on the FUI products during 2019–2021, where outlier values in time series were removed using filter window of the “ $\mu \pm 3\sigma$ ” (μ denotes the average value and σ denotes the standard deviation). In order to cover the main channel (wider than 100 m) of the whole river, 3 years’ data in the same season were used to produce the seasonal maps. Here in the northern hemisphere, spring is from March to May, summer is from June to August, autumn is from September to November, and winter is from December to February in the next year. Then, the seasonal average FUI calculated on the river centerline was used in the analysis.

2.3. In situ datasets

From March to June 2022, three campaigns were conducted in the lower reaches of Yangtze River, through which water-leaving reflectance ($R_{rs}(\lambda)$, sr^{-1}) and water samples were collected. For the $R_{rs}(\lambda)$ collection, the portable spectrometer (ASD FieldSpec®, Analytical Spectral Device, Inc., Boulder, CO, USA) was used to collect the spectra following the “above-water method” (Mueller and Fargion 2002).

In the Danube River, two campaigns were conducted in the Danube Delta during 2015 and 2016, where $R_{rs}(\lambda)$ spectra and water samples sites were collected. Sampling of above water radiometric quantities was carried out using three RAMSES sensors (TriOS GmbH, Germany), which were simultaneously measuring downwelling irradiance (E_d), sky radiance (L_s), and water leaving radiance (L_t). $R_{rs}(\lambda)$ data were processed using fingerprint method first, and then delta corrected (Simis and Olsson 2013). The hyperspectral $R_{rs}(\lambda)$ data collected in field were simulated to the Sentinel-2 MSI bands data using the sensor’s spectral response functions, and the FUI was then calculated from the $R_{rs}(\lambda)$ in Sentinel-2 bands to evaluate the satellite-derived FUI, following the calculation method in Section 2.2 and the evaluation method described in previous studies (Wang et al. 2018, 2021).

A match-up dataset of in-situ data (from Nanjing section of Yangtze River and the Danube Delta) and Sentinel-2 MSI L2A was used in this analysis. A time window of ± 5 days was used. The 3×3 pixel window

FUI colour classes



Figure 1. The 21 water color classes represented in FUI.

was acquired from the images at the location of the sampling sites, and the clouds were masked with the QA60 band as stated in Section 2.1. The center pixel in the 3×3 pixel window was used to match the in-situ R_{rs} (λ) data with a spatial coefficient of variation (CV) less than 0.2 in the 3×3 pixel window. Finally, there were a total of 17 match-ups for Yangtze River and 15 match-ups for Danube River. The location of the sampling sites is shown in Figure 2.

2.4. Environmental auxiliary data

To analyze the potential impact factors on the water color of rivers, the land cover and the meteorological data (including precipitation, air temperature, wind speed) were collected for the two river basins. The land cover data were acquired from the European Space Agency (ESA) WorldCover 2020 product (<https://esa-worldcover.org/>) with global coverage and a resolution of 10 m (Zanaga et al. 2021). The classification method was based on the spectral images of Sentinel-1 and Sentinel-2 spacecraft, with 11 land cover categories. Based on this, the land coverage of each category in

each basin was calculated. The precipitation data were from Climate Hazards Group InfraRed Precipitation with Station dataset (CHIRPS) (<https://www.chc.ucsb.edu/data/chirps/>), with a resolution of 0.05° , which has provided quasi-global rainfall data since 1981 (Funk et al. 2015). The wind speed and temperature data were from the ERA5-Land dataset (<https://www.ecmwf.int/>) with a resolution of 0.1° , which provided the global terrestrial climate data from 1950 to the present (Muñoz-Sabater et al. 2021). Based on the meteorological datasets, the seasonal average values for precipitation, wind speed (at 10 m), and air temperature (at 2 m) in the river basins were calculated. In addition, the water-level data of representative stations in each river basin were obtained from Hydroweb developed by the Theia Scientific Expertise Centre (<https://www.theia-land.fr/en/ceslist/water-levels-of-lakes-and-rivers-sec/>), and the seasonal average water level was calculated from the daily data.

2.5. Spatial and temporal analysis

A series of statistical testing methods were employed to determine whether there are significant changing trends,

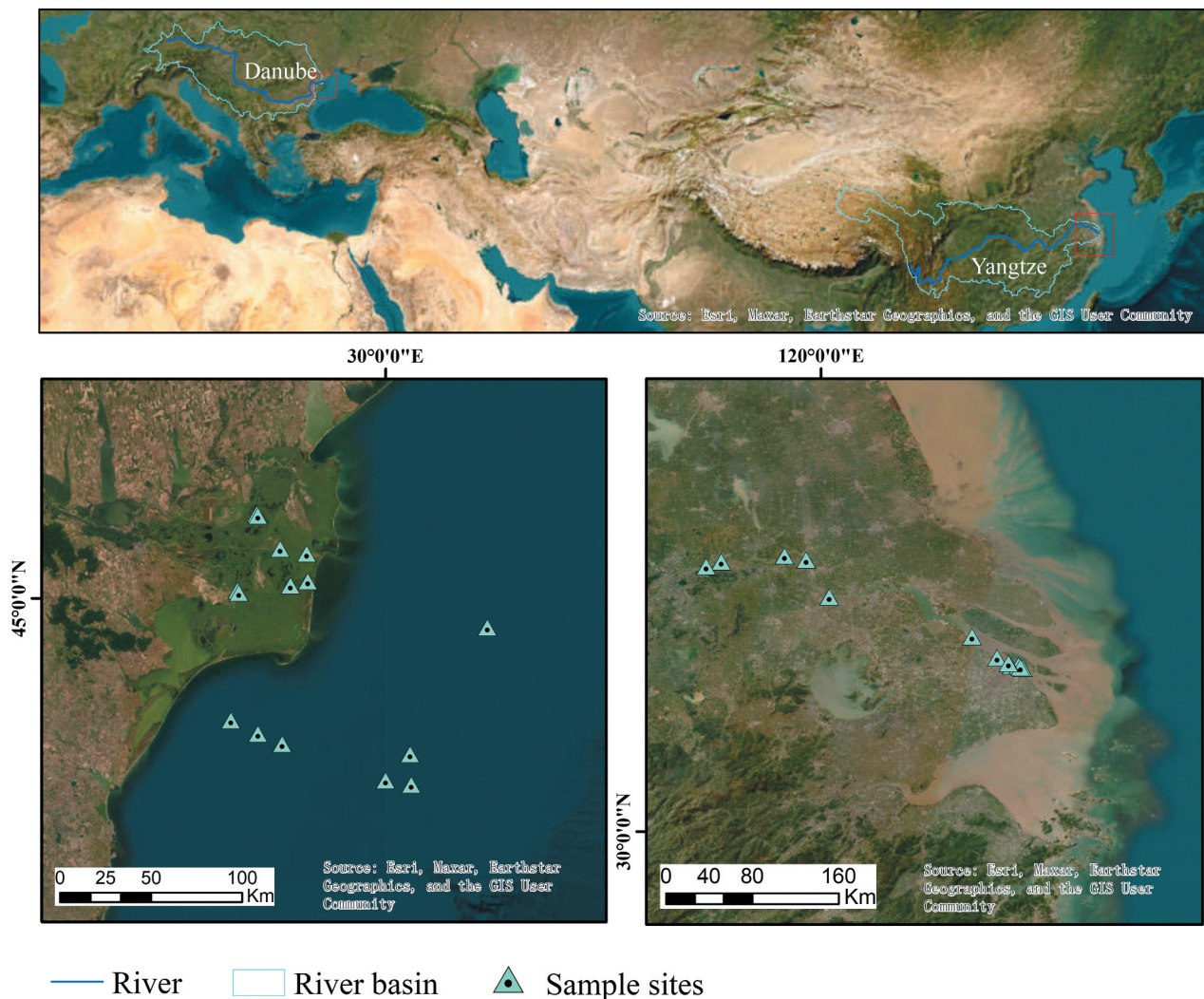


Figure 2. Location of the sampling sites in Danube Delta and the lower reaches of Yangtze River.

statistical differences among river reaches and seasons. First, we used the Shapiro–Wilk (SW) test to assess the normality of the data (Shapiro and Wilk 1965). The results indicated a departure from normality in the FUI data in Yangtze and Danube ($p < 0.05$). Consequently, we applied the Mann–Whitney U (Mann and Whitney 1947) non-parametric test to determine the differences of FUI among seasons and river reaches. The Mann–Whitney U-test does not rely on specific assumptions about the data distribution, making it a widely used method that does not require consideration of the distributional form or known distribution of the data being tested (Kasuya 2001). The Mann–Kendall (MK) trend test method was employed to capture the changing trends of FUI through the rivers (Kendall 1948; Mann 1945). When the MK statistic is greater than 0, it indicates an increasing trend in the variable. Conversely, when the MK statistic is less than 0, it suggests a decreasing trend in the variable. A MK statistic of 0 implies the absence of a trend in the variable. Furthermore, if the absolute value of the MK statistic exceeds 1.96, this trend is considered significant at a 0.05 significance level. In this study, we utilized this method to capture whether there were trends from the source to the mouth in the Yangtze and Danube Rivers during various seasons.

3. Results and discussions

3.1. Validation of water color derivation using Sentinel-2 data

FUI derived from the quasi-synchronous Sentinel-2 and the FUI calculated from the in-situ measured R_{rs} (λ) were used to validate the satellite-derived FUI. As shown in the scatterplots of Figure 3, most of the data points were distributed around the 1:1 line, and the

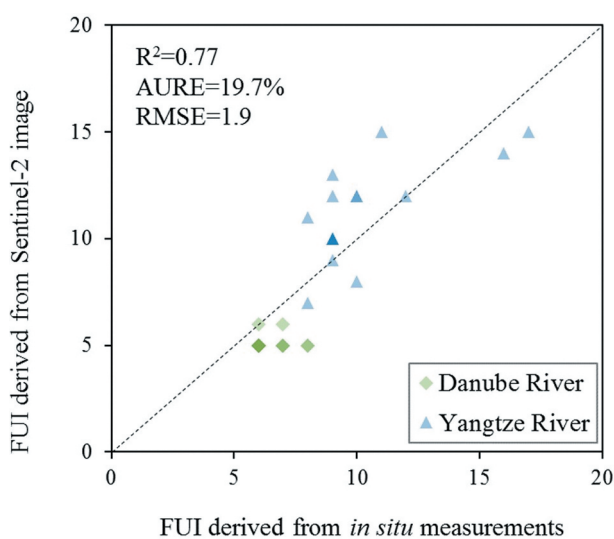


Figure 3. Scatterplots of FUI derived from in-situ measurements and from quasi-synchronous Sentinel-2 images with 17 matchups in Yangtze and 15 matchups in Danube.

satellite-derived FUI and in-situ $R_{rs}(\lambda)$ -derived FUI demonstrate a strong correlation with the R^2 of 0.77, the Average Unbiased Relative Error (AURE) of 19.7%, and the Root Mean Square Error (RMSE) of 1.9. It shows that the relative error of 19.7% is a slightly larger than that ($\sim 10\%$) demonstrated in previous studies where the FUI was derived from MODIS images (Wang et al. 2018, 2021). This is probably because the time matching window was ± 3 h for the daily MODIS data, but it was set ± 5 days here for Sentinel-2 data due to its lower temporal resolution and the scarcity of the in-situ sampling data. Given the dynamic response of river systems to events within the catchment, water color may change considerably during the 5-day window. Moreover, river water generally has higher mobility than lake water since the water is always flowing in rivers and has more connection with the surrounding land. Nevertheless, these results with uncertainties of less than 20% confirmed the reliability of the developed FUI product. To further show the color characterizing ability of the FUI calculation system, the RGB-composited true color and the corresponding calculated FUI image are compared in Figure 4 at several locations in Yangtze and Danube. It can be seen from the figure that the FUI maps generally can remain approximate color with the true color image with small differences that may be due to the FUI classification and the brightness.

3.2. Spatial patterns of water color in Yangtze and Danube

The FUI maps of the Yangtze River in the four seasons during 2019–2021 are illustrated in Figure 5. It can be seen, except in the summer, that the FUI of the Yangtze River gradually increases from the upper reaches to the middle and lower reaches, with significant increasing trends indicated by the MK trend test ($p < 0.05$). This indicates that the Yangtze River gradually becomes turbid as it flows from its upper to lower reaches. But, in summer, there was no significant trend in FUI through Yangtze, and FUI of the upper and middle reaches of the Yangtze River was larger than that in the lower reaches, which may be related to the heavy rainfall and runoff in summer on the steep-sided slopes within the mountainous upper and middle reaches of the Yangtze River catchment (Yang et al. 2015). In the upper reaches of Yangtze, as shown in Figure 5, water color changes dramatically between the four ladder hydropower stations (WDD for Wudongde, BHT for Baihetan, XLD for Xiluodu, and XJB for Xiangjiaba) in the four seasons with the same pattern, where FUI rises fast from the first ladder dam to the second ladder dam, then drops sharply between the second ladder dam and the third, and finally becomes lower in the fourth ladder dam. This might be impacted by the impounding and operation of the four ladder dams constructed in the upstream of Yibin City.

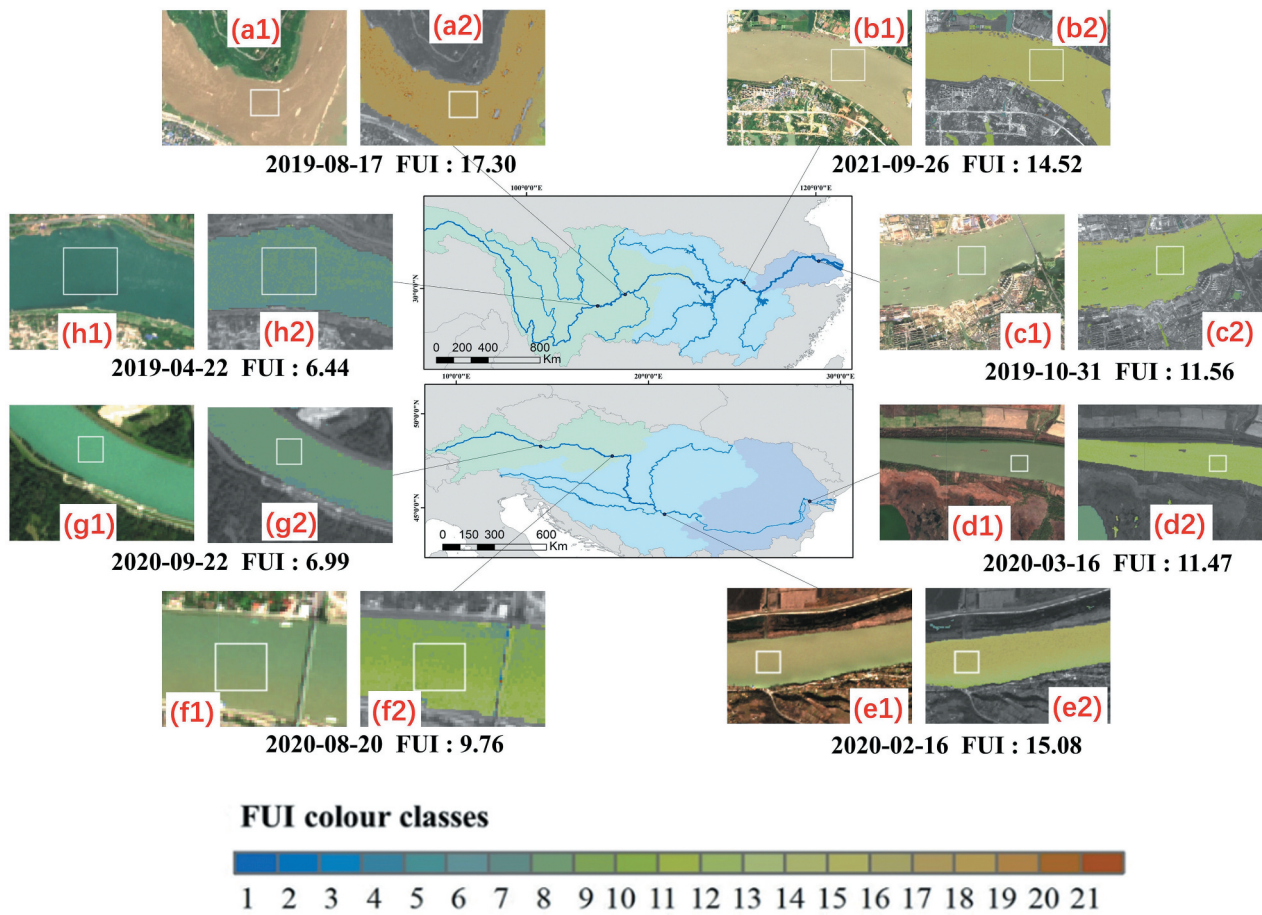


Figure 4. Comparison of the RGB-composited true color image (a1, b1, c1, d1, e1, f1, g1, h1) and the corresponding FUI color image (a2, b2, c2, d2, e2, f2, g2, h2) in Yangtze River and Danube River. The image acquisition date is noted below the image, and the FUI data noted are the averaged FUI value of the pixels enclosed by the white box on the image.

In summer, the deviations between the four dams are very obvious, which is probably because of the flood discharge during the flood season. The FUI also peaks at the Three Gorges Dam (TGD), the largest hydropower station in the Yangtze River, and the lower zone of TGD has a higher FUI than that in the upper zone of TGD in summer, which may also be explained by the flood discharge of the dam during summer. In contrast, in other seasons, the lower zone of TGD has a lower FUI, as the dam generally impounds water from the end of September to the next May (Floehr et al. 2013). In summer of the middle reaches, it can also be found that the FUI presented a valley shape around Lake Dongting (near Yueyang City) and Lake Poyang (near Jiujiang City), the two largest river-connecting lakes of the Yangtze River, which was likely impacted by the water and sediment regulation function of the river-connecting lakes (Jones and Rosenfeld 2010). In the lower reaches, after the merge of the Huaihe River in Yangzhou City, the FUI of the Yangtze River had a slight decline and then rose to high values in the estuary area in Shanghai City.

The FUI maps of the Danube River in the four seasons during 2019–2021 are shown in Figure 6. A direct comparison between the two rivers reveals

that the FUI in Yangtze is generally higher than that in Danube, and the spatial variations of FUI are smaller in magnitude in the Danube River than those observed in the Yangtze River. More importantly, the FUI is increasing from the source to the river mouth in spring and winter, but it is decreasing in summer and autumn with significant decreasing trends, as indicated by the MK trend test ($p < 0.05$). The FUI tends to be lower in the lower reach of Danube in summer and autumn. This is likely to be associated with the sediment sink effect of the Iron Gate Dams, where the FUI peaked upstream of the Iron Gate Dams and turned out to be lower downstream of the dam. In the lower reach of Danube after the Iron Gate Dams, there is a gradual transition to higher values as the river reaches the Danube Delta, which is less dramatic than the transition observed in the estuary of the Yangtze River. Compared to the middle and lower reaches of Danube, the FUI tends to be a little higher in the upper reach, especially in summer and autumn, which seems to be related to the high precipitation and runoff in this course, as it is partly affected by the Atlantic climate and Alpine climate, both characterized by high precipitation, while the middle and lower reaches are generally impacted by the continental

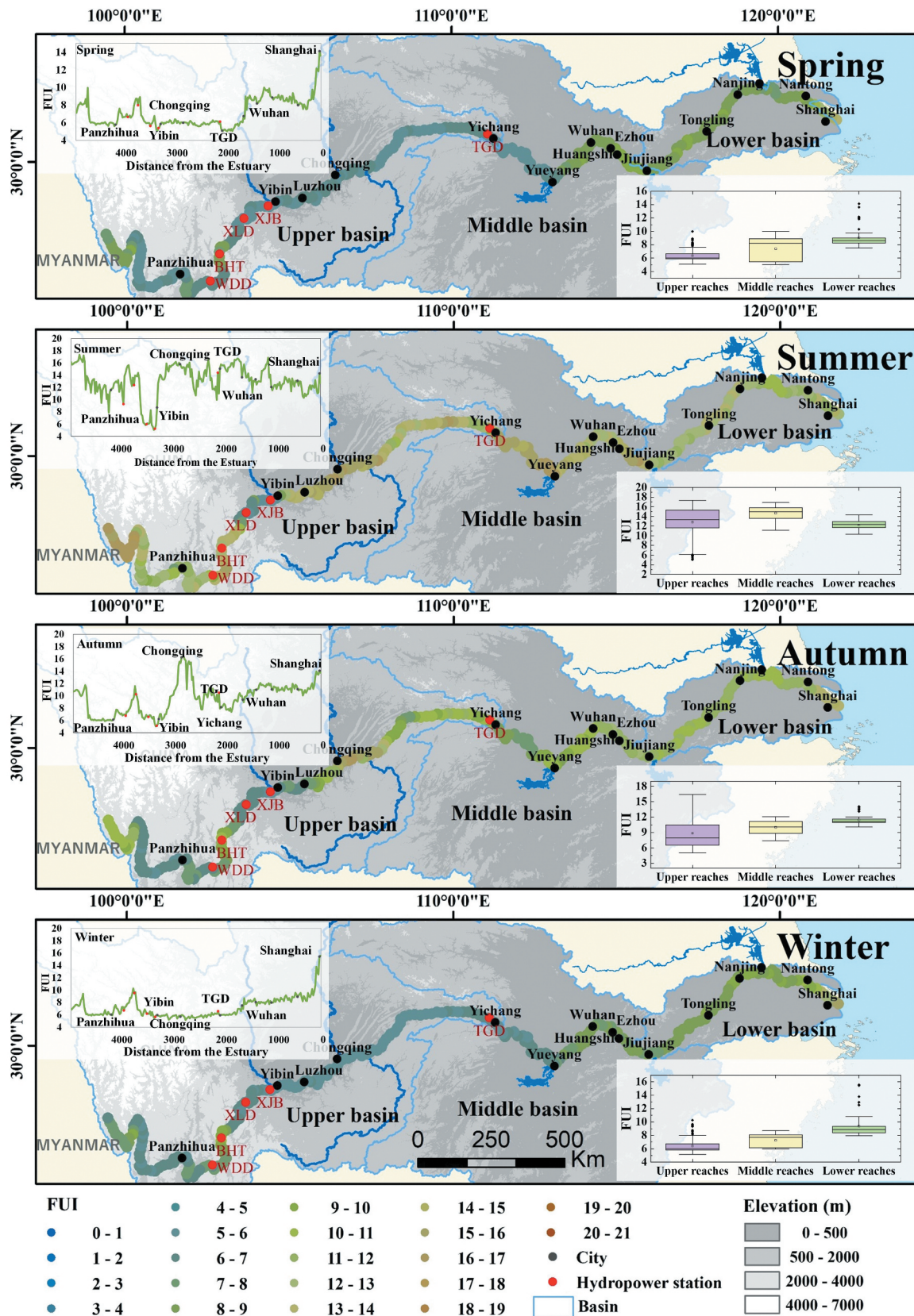


Figure 5. The FUI maps and statistics of Yangtze river in the four seasons during 2019–2021.

climate (Stagl and Hattermann 2015). In addition, variable and contrasting FUI can be found in the Austria course of the river, which might be affected by the operation of the hydropower dams along this course.

3.3. Seasonal variations of water color in Yangtze and Danube

The seasonal variations of FUI in Yangtze and Danube are depicted in Figure 7. The Mann–Whitney U-test

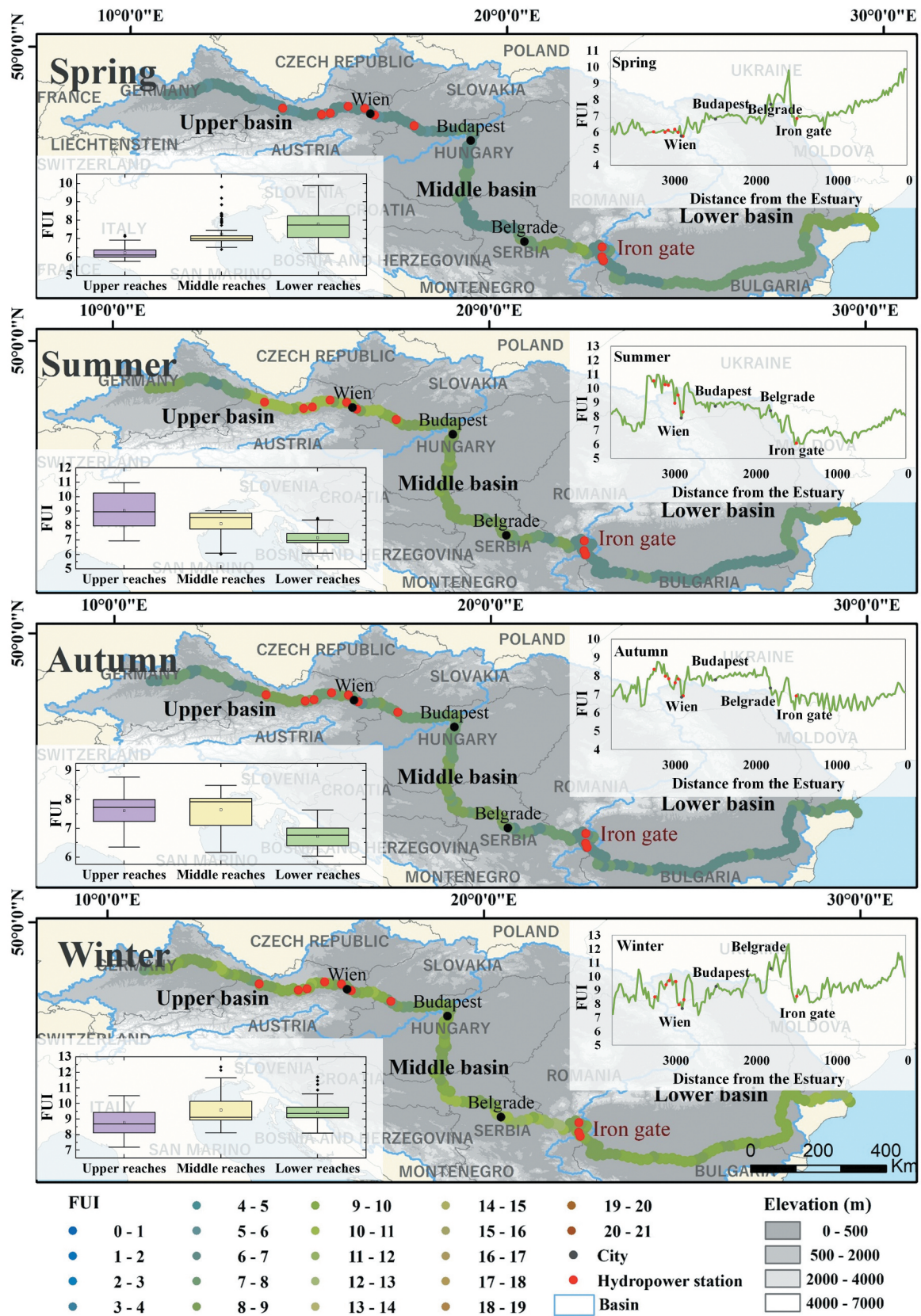


Figure 6. The FUI maps and statistics of the Danube River in the four seasons during 2019–2021.

showed that there were significant seasonal differences between the four seasons ($p < 0.05$), except for the difference between spring and winter. In the non-flood seasons, i.e. spring and winter, FUI for the whole river was generally low with average values of

7.4 and 7.5, and the FUI differences in different reaches were small with a standard deviation of 2.1 and 2.3 for the two seasons, respectively. This shows that the water of the Yangtze River was relatively clean in the non-flood seasons. In contrast, in summer when

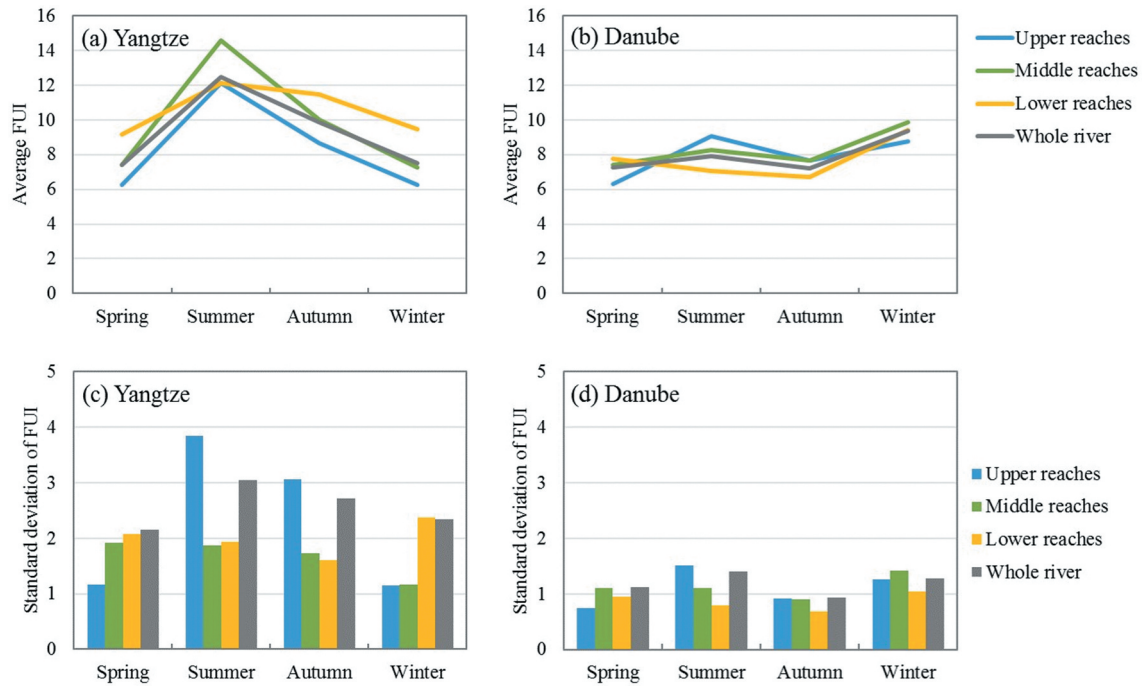


Figure 7. The seasonal variations of FUI in average value and standard deviation of the Yangtze and Danube rivers.

precipitation in the basin is the heaviest in the whole basin, the average FUI of the Yangtze River reached 12.5 indicating that the water is turbid during summer, while the FUI difference in the whole river was relatively large with a standard deviation of 3.1. In summer, the FUI difference of the upper reach was the largest with a standard deviation of 3.8 and an average value of 12.1. The FUI of the middle reach in summer was the highest with an average value of 14.6 and a standard deviation of 1.9. In autumn, the average FUI of the whole river was 9.8, which fell in the middle between the summer and the other two non-flood seasons. Overall, there were distinct seasonal variations of water color throughout the whole river, where it turned to be more turbid in the flood season (i.e. summer) and stay relatively clear in the unflood seasons (i.e. spring and winter).

In the Danube River, the Mann–Whitney U-test showed that there were significant seasonal differences between the four seasons ($p < 0.05$). But the seasonal change line of FUI in the whole river was consistently in a general zigzag shape, and high FUI was found in summer and winter (Figure 6). The winter observed the highest average FUI in the whole river with an average value of 9.3 and a standard deviation of 1.3. The second highest FUI of the whole river was found in summer when the precipitation and water level are the highest in the four seasons. Thereinto, the average FUI in the whole river during summer was 7.9, with a standard deviation of 1.4. It is worth noting that in the upper reaches of Danube, FUI was highest in summer with an average value of 9.1, together with high color variations with a standard deviation of 1.5. This is likely linked to the high precipitation in

summer in the upper basin where summer is the wettest season (Stagl and Hattermann 2015). Low FUI of the whole river was observed in the other two seasons, i.e. spring and autumn, with average values of 7.3 and 7.2 and standard deviation values of 1.1 and 0.9, respectively.

3.4. Environmental factors related to the water color variations in the two rivers

River water can be significantly impacted by the combined effect of climate variability, land cover, and dam construction along the river (Birk et al. 2020; Dethier, Renshaw, and Magilligan 2022; Yang et al. 2015). These factors can further impact the spatial and seasonal changes in water color within rivers.

Hydro-meteorological variability may influence the seasonal water level and water color of the river. The seasonal variations of the hydro-meteorological variables in the two river systems are shown in Figure 7. The climate in the Yangtze River basin is dominated by the subtropical monsoon climate that is characterized by high precipitation, especially in the summer (Yang et al. 2015). The seasonal variations of FUI in the Yangtze generally presented a pattern of a convex curve, i.e. highest in summer and lowest in spring and winter, which is very similar to the seasonal patterns of the water level and precipitation in the basin. This is probably because the high precipitation and runoff in summer will disturb the water in the Yangtze River and bring in more suspended sediment and dissolved matter (Yang et al. 2015). The precipitation in Yangtze basin is also low in autumn, but the FUI of Yangtze in autumn falls in the middle of the summer and the

other two seasons. This is probably linked to the lag effect of precipitation since it takes about 1 month for the precipitation in the basin to enter the main channel of river. The climate conditions in the west–east direction of the Danube River basin are complicated and variable being within transitional zones in temperate oceanic, temperate continental, and Mediterranean climates. The interaction of the three main climates can trigger floods at any period of the year along the Danube (Stagl and Hattermann 2015). However, the water level of Danube and precipitation in the basin presented a pattern of a zigzag curve, i.e. highest in summer and decreases in autumn, which is also generally in the same shape of the seasonal curve of FUI in Danube reaches. This indicates that the water level of river and precipitation in the basin can largely affect the seasonal changes of water color in the river.

Hydropower stations constructed along the river can significantly impact the spatial variations of water color in both rivers. In the Yangtze River, the Three Gorges Dam is the largest hydropower station and is located between the upper and middle reaches of the river, which has been demonstrated to have considerable influences on the river ecosystem and suspended sediment flux of the Yangtze River since its construction in 2003 (Yang et al. 2018). This study indicated that the FUI was generally higher upstream of the dam and lower downstream of the dam during the non-flood seasons (i.e. spring and winter), possibly due to sediment intercepted by the dam impoundment. In turn, the FUI suddenly turned high downstream of the dam during the flood season (i.e. summer), which can be related to the water and sediment discharge of the dam. The ladder hydropower dams constructed in the upper reach of Yangtze also impacted the water and sediment distribution of the river (Yang et al. 2015). We found that the FUI generally decreased as passing through the four ladder dams and increased after the ladder dams when the tributary fed into the river in Yibin City. In Danube, the largest hydropower stations are the Iron Gate I and Iron Gate II dams constructed between the middle and lower reaches of the river in the 1970s. Studies have illustrated that the Iron Gate dams had a significant impact on the sediment movement and continuity along the Danube, contributing to sediment starvation in the Danube Delta (Panin and Jipa 2002; Stănică et al. 2011). We observed that the FUI was lower in the lower reach, which can be attributed to the sediment sink effect of the Iron Gate Dams to a certain degree. Another 187 dams, which are in operation on the Romanian tributaries (Rădoane and Rădoane 2005), may have the same sink effect, contributing further to lowering turbidity in the Lower Danube. In addition, the high spatial variations in the upper reach of Danube during flood seasons (i.e. summer

and winter) are possibly due to the operation of the dense dams in this region.

The land cover within the river basin can also partly contribute to the river water environment and spatial variations of water color in the river. According to the land cover types map of the two river systems based on the ESA WorldCover 2020 product (as shown Figure 8), it showed that the bare/sparse vegetation coverage rates (including the tree cover, grassland, shrubland and cropland) in the upper and lower basins of the Yangtze River consistently reached 7.2% and the middle basin's bare/sparse vegetation coverage rate was still with a high value of 4.6% (Figure 9(a) and Figure 10(a)). In contrast, the bare/sparse vegetation coverage rates in the three basins of the Danube River were much lower with values from 0.7% in the middle basin to 1.2% in the upper basin (Figure 9(b) and Figure 10(b)). Simultaneously, higher levels of built-up coverage rates were found in the middle and lower basins of Yangtze River with values of 3.0% and 7.4%, while the built-up coverage rates in the three Danube River basins were relatively low with values from 1.7% to 3.2% (Figure 10). The land cover differences in the two river basins may explain why the FUI in the Yangtze River is generally higher than that in the Danube River, since runoff in the basin may carry more soil sediments into the river system with higher bare/sparse vegetation coverage rate (Guan et al. 2022; Long et al. 2006). It is also worth noting that the higher elevation difference of Yangtze River from upper to lower reaches, as shown in Figure 5, can also largely contribute to the soil erosion of the river channel and bring more sediments into water (Yang et al. 2015). In addition, the higher levels of precipitation in Yangtze basin compared with that in Danube basin may also exacerbate this difference.

3.5. Implications and uncertainties of water quality observation for rivers with satellite data

The water quality of inland water is critical to human and ecosystem health, food production, and economic growth. Rivers are more sensitive to climate change and the surrounding environment than any other type of inland waters due to their intimate link to the surroundings through various pathways. Consistent and systematic observation of water quality through the river continuum is very necessary to identify the water quality risks and manage the interactions among river, land use, climate change, and other stressors. Satellite observations have been used to assess the water quality variations of rivers, but most of the previous studies were focused on rivers on a regional scale or the estuary regions (Chen, Xiao, and Li 2016; Feng et al. 2014; Miao et al. 2020; Wackerman, Hayden, and Jonik 2017; Yang, Sokoletsky, and Wu 2017; Yang et al. 2023). Owing to the improvement in

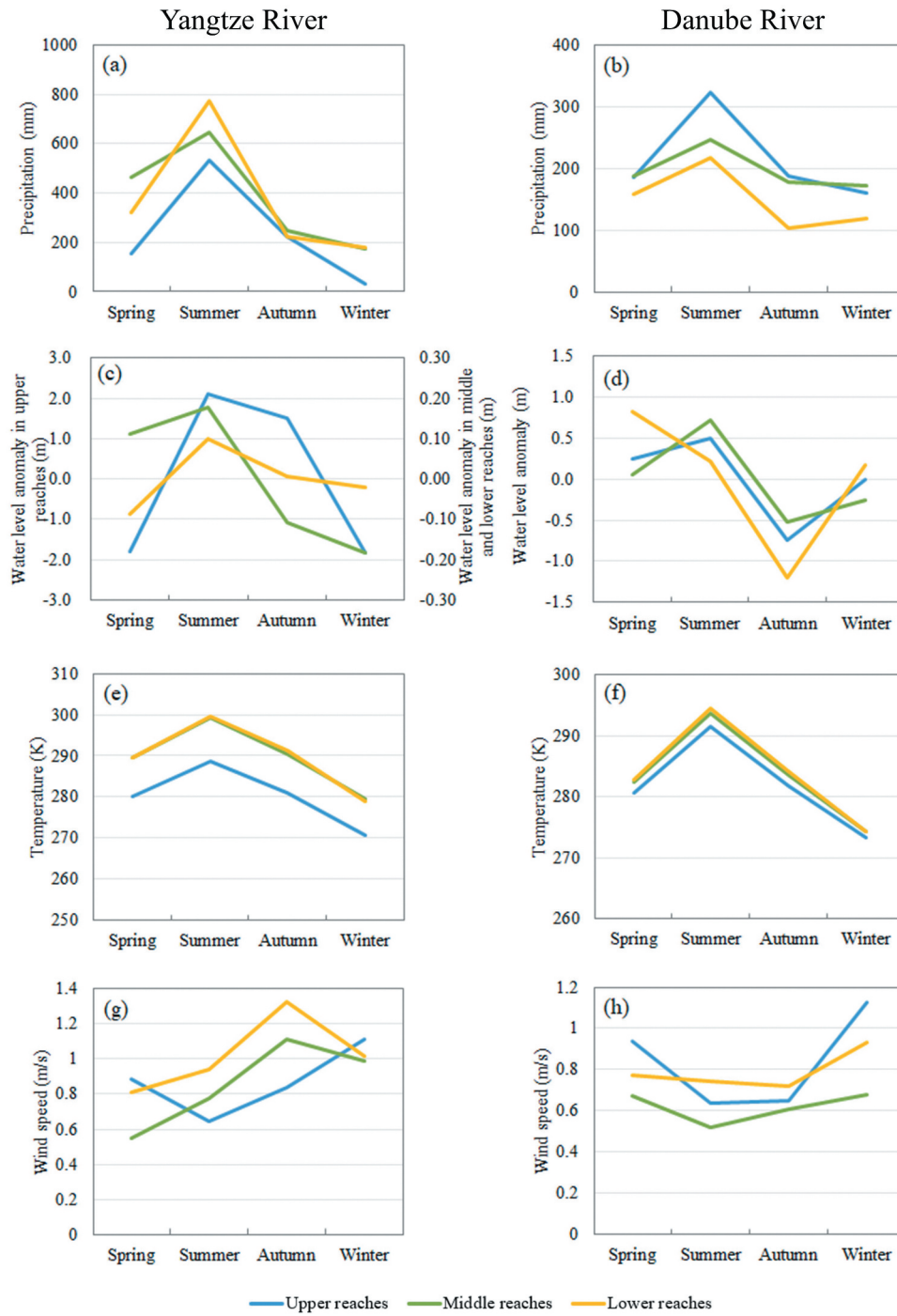


Figure 8. Seasonal variations of the hydro-meteorological variables in the two river systems.

spatial resolution of the satellite data and the progress in water quality remote sensing of inland waters, studies are moving forward to the water quality mapping of the river continuum (Gardner et al. 2021; Guan et al. 2022). However, the water quality retrieval in river continuum is still more challenging than that in lakes and reservoirs due to the enormous spatial difference of water constituents in river continuum (Li et al. 2021; Zhao et al. 2021). In this sense, this study investigated the temporal and spatial patterns of water color in the Yangtze and Danube rivers using FUI, which is an optical indicator of water quality and can be accurately and rapidly derived from satellite data

for wide types of inland waters (Gardner et al. 2021; Wang et al. 2021). The spatial and temporal patterns of water turbidity revealed in this study with FUI in Yangtze were generally consistent with those demonstrated by Zhao et al. (2021) where FUI was used to estimate water clarity in the Yangtze River. “The lower the more turbid” spatial pattern of the Yangtze River was also shown by Li et al. (2021) where the *in situ* measured suspended matter in the Yangtze River was analyzed. As for the turbidity variations in the Danube River, although there was rarely a study on the whole river continuum, studies have indicated the hydro-power stations and numerous dams constructed

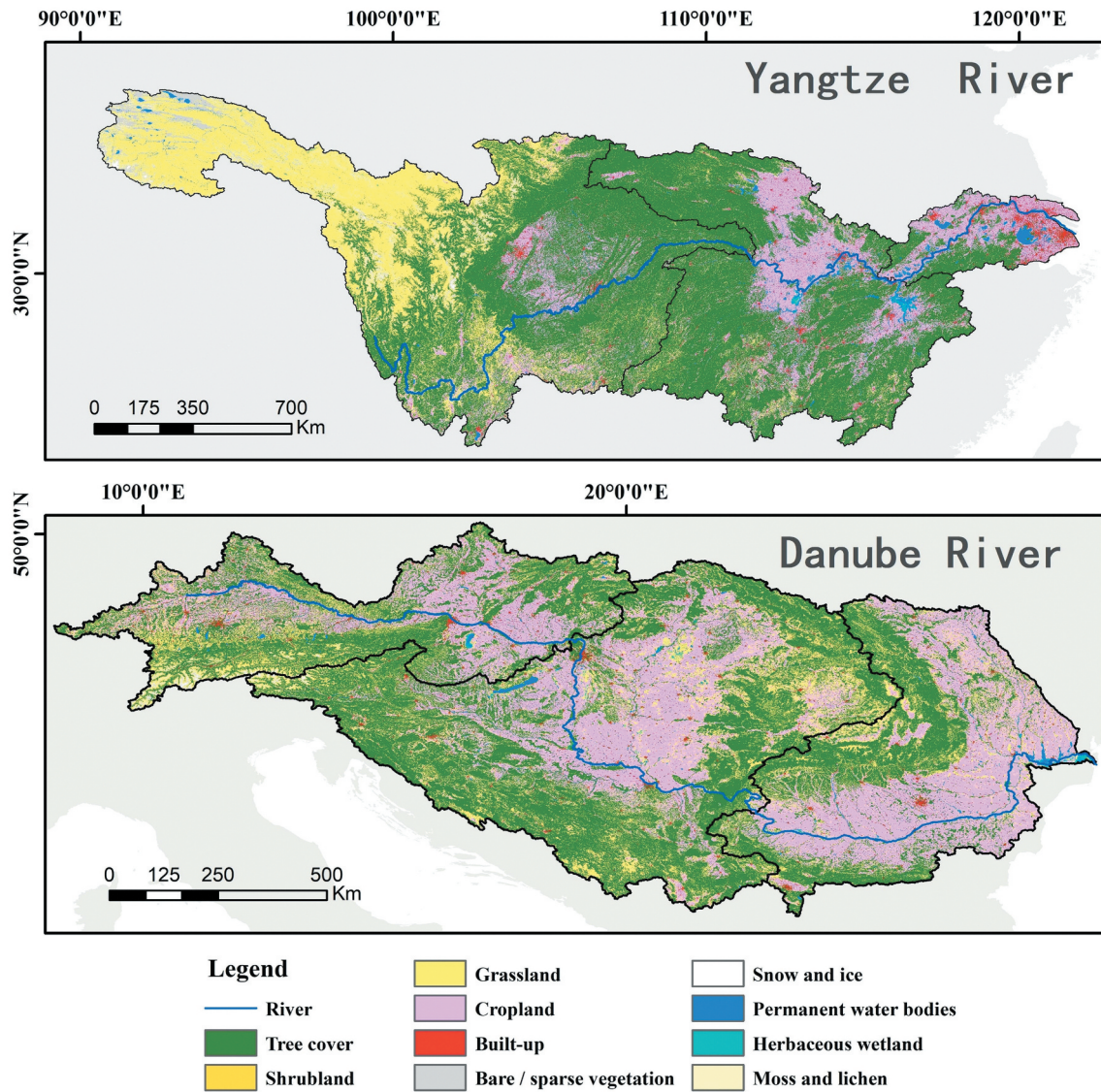


Figure 9. Land cover maps in Yangtze and Danube river basins according to the ESA WorldCover 2020 product.

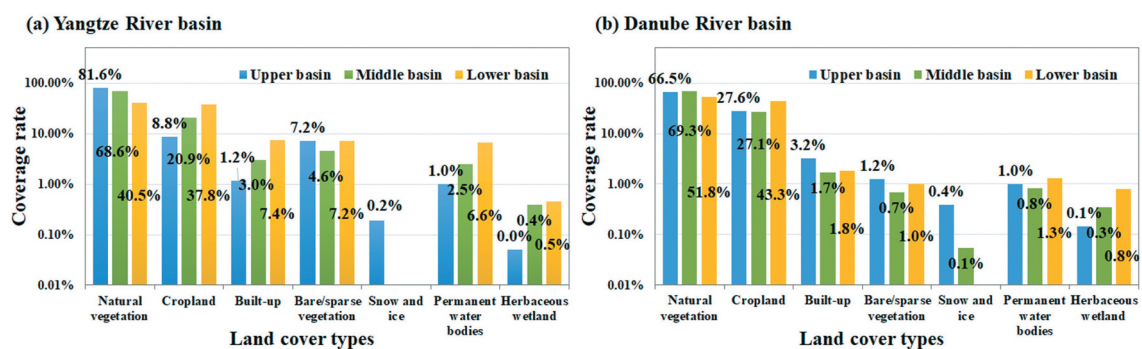


Figure 10. Statistics of the land cover rate of Yangtze and Danube river basins. The vegetation cover includes tree cover, shrubland, grassland and cropland.

along the Danube led to dramatic sediment discharge in the lower reach and river mouth (Constantin, Doxaran, and Constantinescu 2016), which can support the results we found in Danube.

Despite efforts to retrieve accurate FUI across the two rivers, there are still some uncertainties. First of all, the availability of satellite data was unevenly

distributed across different reaches of the river and different seasons due to cloud cover or other un-optimal conditions. To reduce the seasonal and segmental biases in a specific year, we calculated the seasonal average FUI using three years' satellite data during 2019–2021. But more advanced statistical method that consider the distribution of the

satellite data availability in seasons and reaches may help for the satellite observation of water quality of rivers. Second, although studies have demonstrated FUI can be used to indicate comprehensive water quality and water turbidity over a wide range of inland and oceanic waters (Pitarch et al. 2019; Wang et al. 2020), FUI itself is a classification of water color which may have limited capacity in identifying detail differences of water color and water turbidity. In addition, the land adjacency effect is a big problem in satellite observation of water quality in narrow rivers. We extracted the river reaches with width larger than 100 m using the Sentinel-2 data with 10 m resolution, and only pixels on the river centerline were input to calculate FUI, which can largely avoid the land adjacency effect. However, the land adjacency effect remains to be evaluated and corrected for narrower rivers.

4. Conclusions

The increasing monitoring capabilities of recent Earth observation missions have been extending satellite applications to large river systems. Given the complex optical properties and water compositions in the river systems, this study highlights the capacity of FUI, in rapidly quantifying and revealing the spatial variations and seasonality in river channels through the new generation of Earth observation data. As a water color proxy, the FUI was derived in this study for the main channel of the Yangtze and Danube rivers using Sentinel-2 MSI data with relatively high accuracy (~80%). Contrasting water color patterns were observed in the two systems on both the spatial and seasonal scales, and the potential impact factors of the patterns were explored. To sum up, dams and hydropower stations along both river systems and the spatial difference of precipitation have been shown to contribute to spatial variations of FUI due to their impact on sediment flux. By contrasting the water color and land cover in the Yangtze and Danube, we found that the land cover in the river basin may largely determine the water color and turbidity in the river water, as high vegetation coverage in the Danube was associated with lower FUI and water turbidity. As for the seasonal variability of the river water, the high precipitation and floods during the wet season may disturb the river water, resulting in the Yangtze being yellower and more turbid in summer and autumn and the Danube being yellower and more turbid in summer and winter. This study demonstrates that MSI can provide consistent data of water color over the length of rivers and key intelligence on environmental change. These could be used to measure the impacts and benefits of our interventions.

Acknowledgments

We would like to thank Professor Yunmei Li from Nanjing Normal University for providing the *in situ* data in the Yangtze River, and the European Space Agency for providing the Sentinel-2 MSI data. The field work in the Danube Delta is part of the AMC PhD work, jointly funded by GeoEcoMar and the University of Stirling, with support from several projects: ReCoReD (Reconstructing the Changing Impact of the Danube on the Black Sea and Coastal Region), funded by TNA FP7 EuroFleets 2, and PN 09 41 03 02, PN09 41 03 04, PN 16 45 01 04, PN18 16 01 02, PN 19 20 02 01 – Romanian Core Program for Research, funded by the Romanian Government. No potential conflict of interest was reported by the author(s).

Disclosure statement

No potential conflict of interest was reported by the author(s).

Funding

This research has been jointly sponsored by the Dragon 5 Cooperation (grant number 59193), the International Partnership Program of Chinese Academy of Sciences (grant number 313GJHZ2022085FN), and the European Union's Horizon Europe research and innovation programme project DANUBE4all (grant number 101093985). The Director Fund of the International Research Center of Big Data for Sustainable Development Goals (Grant No. CBAS2022DF004).

Notes on contributors

Shenglei Wang is an Associate Professor in Aerospace Information Research Institute, Chinese Academy of Sciences. Her research interest includes water optical remote sensing, bio-optical properties and radiative transfer process in optically-complex waters, and spatio-temporal change analysis of water color and the responses to climate change.

Xuezhu Jiang received a bachelor's degree from Lanzhou University in 2018. Her research interests include optical remote sensing of inland water, analysis of spatiotemporal changes in water quality in optically complex waters, and responses to climate change.

Evangelos Spyarakos is an Associate Professor in Earth observation at University of Stirling. His formal education is in Applied Physics (PhD, 2012 & MSc, 2009) and Marine Sciences (MSc, 2007 & BSc, 2005). His research is primarily focused on remote sensing, light propagation and light-matter interaction in natural aquatic systems in the context of environmental change, scientific/technological innovation and its integration into effective interventions and solutions.

Junsheng Li is a Professor in Aerospace Information Research Institute, Chinese Academy of Sciences. His research interest is optical remote sensing of inland and coastal waters.

Conor McGlinchey is a Dragon 5 Young Scientist currently working on his PhD at the University of Stirling. His research is focused on the development of new satellite products to characterise and monitor phytoplankton properties from space. Prior to starting his PhD, Conor completed his MSc in Geospatial Mapping Sciences at the University of Glasgow.

Adriana Maria Constantinescu received her PhD degree in 2020 from the University of Stirling. She is a researcher at GeoEcoMar, Romania. Her work focuses on water quality, the dynamics and forcing factors of water and sediment fluxes in the Danube-Danube Delta- Black Sea System, education and science communication.

Andrew N. Tyler is a Professor in Environmental Sciences, and Scotland Hydro Nation Chair in Scotland's International Environment Centre at the University of Stirling. He is also the academic Director for Scotland's International Environment Centre, with a mission to drive inclusive growth and support the net zero carbon agenda by bringing the environment to the heart of decision making. His research team are pioneering in transforming the use of Earth observation technologies for quantifying water quality and quantity at local and global scales.

ORCID

Shenglei Wang  <http://orcid.org/0009-0007-5699-6483>
 Evangelos Spyarakos  <http://orcid.org/0000-0001-7970-5211>
 Junsheng Li  <http://orcid.org/0000-0002-8590-9736>
 Adriana Maria Constantinescu  <http://orcid.org/0000-0001-7768-9385>
 Andrew N. Tyler  <http://orcid.org/0000-0003-0604-5827>

Data availability statement

The data that support the findings of this study are available from the corresponding author, upon reasonable request.

References

- Birk, S., D. Chapman, L. Carvalho, B. M. Spears, H. E. Andersen, C. Argillier, S. Auer, A. Baattrup-Pedersen, L. Banin, and M. Beklioglu. 2020. "Impacts of Multiple Stressors on Freshwater Biota Across Spatial Scales and Ecosystems." *Nature Ecology & Evolution* 4 (8): 1060–1068. <https://doi.org/10.1038/s41559-020-1216-4>.
- Cao, Z., M. Shen, T. Kutser, M. Liu, T. Qi, J. Ma, R. Ma, and H. Duan. 2022. "What Water Color Parameters Could Be Mapped Using MODIS Land Reflectance Products: A Global Evaluation Over Coastal and Inland Waters." *Earth-Science Reviews* 232:104154. <https://doi.org/10.1016/j.earscirev.2022.104154>.
- Chen, F., D. Xiao, and Z. Li. 2016. "Developing Water Quality Retrieval Models with in situ Hyperspectral Data in Poyang Lake, China." *Geo-Spatial Information Science* 19 (4): 12. <https://doi.org/10.1080/10095020.2016.1258201>.
- Constantin, S., D. Doxaran, and Ş. Constantinescu. 2016. "Estimation of Water Turbidity and Analysis of Its Spatio-Temporal Variability in the Danube River Plume (Black Sea) Using MODIS Satellite Data." *Continental Shelf Research* 112:14–30. <https://doi.org/10.1016/j.csr.2015.11.009>.
- Constantinescu, Ş., D. Achim, I. Rus, and L. Giosan. 2015. "Embanking the Lower Danube: From Natural to Engineered Floodplains and Back." *Geomorphic Approaches to Integrated Floodplain Management of Lowland Fluvial Systems in North America and Europe* 265–288. New York, NY: Springer New York.
- Coss, S. P., M. Durand, C. Shum, Y. Yi, X. Yang, T. M. Pavelsky, A. Getirana, and D. Yamazaki. 2022. "Channel Water Storage Anomalies: A New Remotely Sensed Measurement for Global River Analysis." *Geophysical Research Letters* 50 (1).
- Dethier, E. N., C. E. Renshaw, and F. J. Magilligan. 2022. "Rapid Changes to Global River Suspended Sediment Flux by Humans." *Science* 376 (6600): 1447–1452. <https://doi.org/10.1126/science.abn7980>.
- Feng, L., C. Hu, X. Chen, and Q. Song. 2014. "Influence of the Three Gorges Dam on Total Suspended Matters in the Yangtze Estuary and Its Adjacent Coastal Waters: Observations from MODIS." *Remote Sensing of Environment* 140:779–788. <https://doi.org/10.1016/j.rse.2013.10.002>.
- Floehr, T., H. Xiao, B. Scholz-Starke, L. Wu, J. Hou, D. Yin, X. Zhang, R. Ji, X. Yuan, and R. Ottermanns. 2013. "Solution by Dilution?—A Review on the Pollution Status of the Yangtze River." *Environmental Science and Pollution Research* 20 (10): 6934–6971. <https://doi.org/10.1007/s11356-013-1666-1>.
- Funk, C., P. Peterson, M. Landsfeld, D. Pedreros, J. Verdin, S. Shukla, G. Husak, J. Rowland, L. Harrison, and A. Hoell. 2015. "The Climate Hazards Infrared Precipitation with Stations—A New Environmental Record for Monitoring Extremes." *Scientific Data* 2 (1): 1–21. <https://doi.org/10.1038/sdata.2015.66>.
- Garaba, S. P., A. Friedrichs, D. Voß, and O. Zielinski. 2015. "Classifying Natural Waters with the Forel-Ule Colour Index System: Results, Applications, Correlations and Crowdsourcing." *International Journal of Environmental Research and Public Health* 12 (12): 16096–16109. <https://doi.org/10.3390/ijerph121215044>.
- Gardner, J. R., X. Yang, S. N. Topp, M. R. Ross, E. H. Altenau, and T. M. Pavelsky. 2021. "The Color of Rivers." *Geophysical Research Letters* 48 (1): e2020GL088946. <https://doi.org/10.1029/2020GL088946>.
- Guan, Q., L. Feng, J. Tang, E. Park, T. A. Ali, and Y. Zheng. 2022. "Trends in River Total Suspended Sediments Driven by Dams and Soil Erosion: A Comparison Between the Yangtze and Mekong Rivers." *Water Resources Research* 58 (10): e2022WR031979. <https://doi.org/10.1029/2022WR031979>.
- Habersack, H., T. Hein, A. Stanica, I. Liska, R. Mair, E. Jäger, C. Hauer, and C. Bradley. 2016. "Challenges of River Basin Management: Current Status Of, and Prospects For, the River Danube from a River Engineering Perspective." *Science of the Total Environment* 543:828–845. <https://doi.org/10.1016/j.scitotenv.2015.10.123>.
- Hein, T., U. Schwarz, H. Habersack, I. Nichersu, S. Preiner, N. Willby, and G. Weigelhofer. 2016. "Current Status and Restoration Options for Floodplains Along the Danube River." *Science of the Total Environment* 543:778–790. <https://doi.org/10.1016/j.scitotenv.2015.09.073>.
- Hou, X., L. Feng, Y. Dai, C. Hu, L. Gibson, J. Tang, Z. Lee, Y. Wang, X. Cai, and J. Liu. 2022. "Global Mapping Reveals Increase in Lacustrine Algal Blooms Over the Past Decade." *Nature Geoscience* 15 (2): 130–134. <https://doi.org/10.1038/s41561-021-00887-x>.
- Jones, N. E., and J. Rosenfeld. 2010. "Incorporating Lakes within the River Discontinuum: Longitudinal Changes in Ecological Characteristics in Stream–Lake Networks." *Canadian Journal of Fisheries and Aquatic Sciences* 67 (8): 1350–1362. <https://doi.org/10.1139/F10-069>.
- Kasuya, E. 2001. "Mann–Whitney U Test When Variances are Unequal." *Animal Behaviour* 61 (6): 1247–1249. <https://doi.org/10.1006/anbe.2001.1691>.

- Kendall, M. G. 1948. *Rank Correlation Methods*. Oxford, England: Griffin.
- Li, J., C. Huang, Y. Zha, C. Wang, N. Shang, and W. Hao. 2021. "Spatial Variation Characteristics and Remote Sensing Retrieval of Total Suspended Matter in Surface Water of the Yangtze River." *Environmental Sciences: An International Journal of Environmental Physiology and Toxicology* 42 (11): 5239–5249.
- Li, J., S. Wang, Y. Wu, B. Zhang, X. Chen, F. Zhang, Q. Shen, D. Peng, and L. Tian. 2016. "MODIS Observations of Water Color of the Largest 10 Lakes in China Between 2000 and 2012." *International Journal of Digital Earth* 9 (8): 788–805. <https://doi.org/10.1080/17538947.2016.1139637>.
- Long, H., G. Heilig, J. Wang, X. Li, M. Luo, X. Wu, and M. Zhang. 2006. "Land Use and Soil Erosion in the Upper Reaches of the Yangtze River: Some Socio-Economic Considerations on China's Grain-For-Green Programme." *Land Degradation & Development* 17 (6): 589–603. <https://doi.org/10.1002/ldr.736>.
- Mann, H. B. 1945. "Nonparametric Tests Against Trend." *Econometrica: Journal of the Econometric Society* 13 (3): 245–259. <https://doi.org/10.2307/1907187>.
- Mann, H. B., and D. R. Whitney. 1947. "On a Test of Whether One of Two Random Variables is Stochastically Larger Than the Other." *Annals of Mathematical Statistics* 18 (1): 50–60. <https://doi.org/10.1214/aoms/1177730491>.
- Miao, S., C. Liu, B. Qian, and Q. Miao. 2020. "Remote Sensing-Based Water Quality Assessment for Urban Rivers: A Study in Linyi Development Area." *Environmental Science and Pollution Research* 27 (28): 34586–34595. <https://doi.org/10.1007/s11356-018-4038-z>.
- Mueller, J. L., and G. S. Fargion. 2002. *Ocean Optics Protocols for Satellite Ocean Color Sensor Validation, Revision 3*. Vol. 210004. National Aeronautics and Space Administration, Goddard Space Flight Center.
- Muñoz-Sabater, J., E. Dutra, A. Agustí-Panareda, C. Albergel, G. Arduini, G. Balsamo, S. Boussetta, M. Choulga, S. Harrigan, and H. Hersbach. 2021. "ERA5-Land: A State-of-the-Art Global Reanalysis Dataset for Land Applications." *Earth System Science Data* 13 (9): 4349–4383. <https://doi.org/10.5194/essd-13-4349-2021>.
- Otsu, N. 1979. "A Threshold Selection Method from Gray-Level Histograms." *IEEE Transactions on Systems, Man, and Cybernetics* 9 (1): 62–66. <https://doi.org/10.1109/TSMC.1979.4310076>.
- Panin, N., and D. Jipa. 2002. "Danube River Sediment Input and Its Interaction with the North-Western Black Sea." *Estuarine, Coastal and Shelf Science* 54 (3): 551–562. <https://doi.org/10.1006/ecss.2000.0664>.
- Panin, N., and W. Overmars. 2012. "The Danube Delta Evolution During the Holocene: Reconstruction Attempt Using Geomorphological and Geological Data and Some of the Existing Cartographic Documents." *GeoEcoMarina* 18:75–104.
- Pitarch, J., H. J. van der Woerd, R. J. Brewin, and O. Zielinski. 2019. "Optical Properties of Forel-Ule Water Types Deduced from 15 Years of Global Satellite Ocean Color Observations." *Remote Sensing of Environment* 231:111249. <https://doi.org/10.1016/j.rse.2019.111249>.
- Pitarch, J., M. Bellacicco, S. Marullo, and H. J. Van Der Woerd. 2021. "Global Maps of Forel-Ule Index, Hue Angle and Secchi Disk Depth Derived from 21 Years of Monthly ESA Ocean Colour Climate Change Initiative Data." *Earth System Science Data* 13 (2): 481–490. <https://doi.org/10.5194/essd-13-481-2021>.
- Qiu, Y. 2018. "Global River and Lake Vector Dataset (2010)." Beijing: National Tibetan Plateau/Third Pole Environment Data Center.
- Rădoane, M., and N. Rădoane. 2005. "Dams, Sediment Sources and Reservoir Silting in Romania." *Geomorphology* 71 (1–2): 112–125. <https://doi.org/10.1016/j.geomorph.2004.04.010>.
- Reid, A. J., A. K. Carlson, I. F. Creed, E. J. Eliason, P. A. Gell, P. T. Johnson, K. A. Kidd, T. J. MacCormack, J. D. Olden, and S. J. Ormerod. 2019. "Emerging Threats and Persistent Conservation Challenges for Freshwater Biodiversity." *Biological Reviews* 94 (3): 849–873. <https://doi.org/10.1111/brv.12480>.
- Schwarz, U., M. Babic-Mladenovic, C. Bondar, G. Gergov, K. Holubova, S. Modev, L. Rákóczi, G. Rast, J. Steindl, and T. Sorin. 2008. "Assessment of the Balance and Management of Sediments of the Danube Waterway—Current Status, Problems and Recommendations for Action." *World Wide Fund for Nature, Vienna*.
- Shapiro, S. S., and M. B. Wilk. 1965. "An Analysis of Variance Test for Normality (Complete Samples)." *Biometrika* 52 (3/4): 591–611. <https://doi.org/10.1093/biomet/52.3-4.591>.
- Simis, S. G., and J. Olsson. 2013. "Unattended Processing of Shipborne Hyperspectral Reflectance Measurements." *Remote Sensing of Environment* 135: 202–212.
- Sommerwerk, N., J. Bloesch, C. Baumgartner, T. Bittl, D. Čerba, B. Csányi, G. Davideanu, M. Dokulil, G. Frank, and I. Grecu. 2022. "The Danube River Basin." In *Rivers of Europe*, 81–180. Elsevier.
- Stagl, J. C., and F. F. Hattermann. 2015. "Impacts of Climate Change on the Hydrological Regime of the Danube River and Its Tributaries Using an Ensemble of Climate Scenarios." *Water* 7 (11): 6139–6172. <https://doi.org/10.3390/w7116139>.
- Stănică, A., S. Dan, J. A. Jiménez, and G. V. Ungureanu. 2011. "Dealing with Erosion Along the Danube Delta Coast. The CONSCIENCE Experience Towards a Sustainable Coastline Management." *Ocean & Coastal Management* 54 (12): 898–906. <https://doi.org/10.1016/j.ocecoaman.2011.06.006>.
- Vadineanu, A., M. Adamescu, R. Vadineanu, S. Cristofor, and C. Negrei. 2003. "Past and Future Management of Lower Danube Wetlands System: A Bioeconomic Appraisal." *Journal of Interdisciplinary Economics* 14 (4): 415–447. <https://doi.org/10.1177/02601079X03001400407>.
- Van der Woerd, H. J., and M. R. Wernand. 2015. "True Colour Classification of Natural Waters with Medium-Spectral Resolution Satellites: SeaWiFS, MODIS, MERIS and OLCI." *Sensors* 15 (10): 25663–25680. <https://doi.org/10.3390/s151025663>.
- Van der Woerd, H. J., and M. R. Wernand. 2018. "Hue-Angle Product for Low to Medium Spatial Resolution Optical Satellite Sensors." *Remote Sensing* 10 (2): 180. <https://doi.org/10.3390/rs10020180>.
- Wackerman, C., A. Hayden, and J. Jonik. 2017. "Deriving Spatial and Temporal Context for Point Measurements of Suspended-Sediment Concentration Using Remote-Sensing Imagery in the Mekong Delta." *Continental Shelf Research* 147:231–245. <https://doi.org/10.1016/j.csr.2017.08.007>.
- Wang, S., J. Li, Q. Shen, B. Zhang, F. Zhang, and Z. Lu. 2014. "MODIS-Based Radiometric Color Extraction and Classification of Inland Water with the Forel-Ule Scale: A Case Study of Lake Taihu." *IEEE Journal of Selected Topics in Applied Earth Observations & Remote Sensing* 8 (2): 907–918. <https://doi.org/10.1109/JSTARS.2014.2360564>.

- Wang, S., J. Li, B. Zhang, Z. Lee, E. Spyrakos, L. Feng, C. Liu, H. Zhao, Y. Wu, and L. Zhu. 2020. "Changes of Water Clarity in Large Lakes and Reservoirs Across China Observed from Long-Term MODIS." *Remote Sensing of Environment* 247:111949. <https://doi.org/10.1016/j.rse.2020.111949>.
- Wang, S., J. Li, B. Zhang, Q. Shen, F. Zhang, and Z. Lu. 2016. "A Simple Correction Method for the MODIS Surface Reflectance Product Over Typical Inland Waters in China." *International Journal of Remote Sensing* 37 (24): 6076–6096. <https://doi.org/10.1080/01431161.2016.1256508>.
- Wang, S., J. Li, B. Zhang, E. Spyrakos, A. N. Tyler, Q. Shen, F. Zhang, T. Kuster, M. K. Lehmann, and Y. Wu. 2018. "Trophic State Assessment of Global Inland Waters Using a MODIS-Derived Forel-Ule Index." *Remote Sensing of Environment* 217:444–460. <https://doi.org/10.1016/j.rse.2018.08.026>.
- Wang, S., J. Li, W. Zhang, C. Cao, F. Zhang, Q. Shen, X. Zhang, and B. Zhang. 2021. "A Dataset of Remote-Sensed Forel-Ule Index for Global Inland Waters During 2000–2018." *Scientific Data* 8 (1): 26. <https://doi.org/10.1038/s41597-021-00807-z>.
- Wang, Y., L. Liu, Y. Hu, D. Li, and Z. Li. 2016. "Development and Validation of the Landsat-8 Surface Reflectance Products Using a MODIS-Based Per-Pixel Atmospheric Correction Method." *International Journal of Remote Sensing* 37 (6): 1291–1314. <https://doi.org/10.1080/01431161.2015.1104742>.
- Xu, H. 2005. "A Study on Information Extraction of Water Body with the Modified Normalized Difference Water Index (MNDWI)." *Journal of Remote Sensing* 9 (5): 595.
- Yang, G., L. Weng, L. Li, L. Gu, and C. Ma. 2008. *Yangtze Conservation and Development Report 2007*. Wuhan, China: Science Press.
- Yang, H., S. Yang, K. Xu, J. Milliman, H. Wang, Z. Yang, Z. Chen, and C. Zhang. 2018. "Human Impacts on Sediment in the Yangtze River: A Review and New Perspectives." *Global and Planetary Change* 162:8–17. <https://doi.org/10.1016/j.gloplacha.2018.01.001>.
- Yang, S., J. Lu, X. Chen, X. Hou, Z. Wei, and J. Wu. 2023. "Unraveling Environmental Influences on the Spatial and Temporal Dynamics of Cyanobacterial Blooms in Lake Erhai During Its Early Stage of Eutrophication." *Geo-Spatial Information Science* 1–19. <https://doi.org/10.1080/10095020.2023.2217860>.
- Yang, S., K. Xu, J. Milliman, H. Yang, and C. Wu. 2015. "Decline of Yangtze River Water and Sediment Discharge: Impact from Natural and Anthropogenic Changes." *Scientific Reports* 5 (1): 12581. <https://doi.org/10.1038/srep12581>.
- Yang, X., T. M. Pavelsky, G. H. Allen, and G. Donchyts. 2019. "RivWidthcloud: An Automated Google Earth Engine Algorithm for River Width Extraction from Remotely Sensed Imagery." *IEEE Geoscience and Remote Sensing Letters* 17 (2): 217–221. <https://doi.org/10.1109/LGRS.2019.2920225>.
- Yang, X., L. Sokoletsky, and H. Wu. 2017. "Water Quality Seasonal Variability (2000 to 2015) in Yangtze River Estuary and Its Adjacent Coastal Area." *J Remote Sensing & GIS* 6 (216): 2.
- Yin, Z., J. Li, Y. Liu, Y. Xie, F. Zhang, S. Wang, X. Sun, and B. Zhang. 2021. "Water Clarity Changes in Lake Taihu Over 36 Years Based on Landsat TM and OLI Observations." *International Journal of Applied Earth Observation and Geoinformation* 102:102457. <https://doi.org/10.1016/j.jag.2021.102457>.
- Zanaga, D., R. Van De Kerchove, W. De Keersmaecker, N. Souverijns, C. Brockmann, R. Quast, J. Wevers, A. Grosu, A. Paccini, and S. Vergnaud. 2021. "ESA WorldCover 10 M 2020 v100." *Zenodo*.
- Zhang, W., S. Wang, B. Zhang, F. Zhang, Q. Shen, Y. Wu, Y. Mei, R. Qiu, and J. Li. 2022. "Analysis of the Water Color Transitional Change in Qinghai Lake During the Past 35 Years Observed from Landsat and MODIS." *Journal of Hydrology: Regional Studies* 42:101154. <https://doi.org/10.1016/j.ejrh.2022.101154>.
- Zhao, Y., S. Wang, F. Zhang, Q. Shen, and J. Li. 2021. "Retrieval and Spatio-Temporal Variations Analysis of Yangtze River Water Clarity from 2017 to 2020 Based on Sentinel-2 Images." *Remote Sensing* 13 (12): 2260. <https://doi.org/10.3390/rs13122260>.